On-the-Fly *Ab Initio* Semiclassical Evaluation of Electronic Coherences in Polyatomic Molecules Reveals a Simple Mechanism of Decoherence

Nikolay V. Golubev[*], Tomislav Begušić, and Jiří Vaníček[†]

Laboratory of Theoretical Physical Chemistry, Institut des Sciences et Ingénierie Chimiques,
Ecole Polytechnique Fédérale de Lausanne (EPFL), CH-1015 Lausanne, Switzerland

Irradiation of a molecular system by an intense laser field can trigger dynamics of both electronic and nuclear subsystems. The lighter electrons usually move on much faster, attosecond timescale but the slow nuclear rearrangement damps ultrafast electronic oscillations, leading to the decoherence of the electronic dynamics within a few femtoseconds. We show that a simple, single-trajectory semiclassical scheme can evaluate the electronic coherence time in polyatomic molecules accurately by demonstrating an excellent agreement with full-dimensional quantum calculations. In contrast to numerical quantum methods, the semiclassical one reveals the physical mechanism of decoherence beyond the general blame on nuclear motion. In the propiolic acid, the rate of decoherence and the large deviation from the static frequency of electronic oscillations are quantitatively described with just two semiclassical parameters—the phase space distance and signed area between the trajectories moving on two electronic surfaces. Because it evaluates the electronic structure on the fly, the semiclassical technique avoids the "curse of dimensionality" and should be useful for preselecting molecules for experimental studies.

Recent progress in laser technologies [1–3] has revolutionized the field of atomic and molecular physics. In particular, tremendous developments of coherent light sources enabled the creation of subfemtosecond laser pulses with remarkably well controlled parameters [4]. Using state-of-the-art lasers, one is able to initiate and probe processes that are driven solely by the electron correlation, i.e., to study and manipulate electron dynamics on its natural timescale [5].

Experimental measurements of the electron motion in isolated atoms were reported [6,7], whereas a direct evidence of ultrafast electron dynamics in molecules remains a point of debate [8]. In particular, there are contradictions between recent experimental studies [9,10] claiming to have observed the ultrafast electronic processes in molecules and theoretical investigations [11,12] performed on systems of similar complexity. The disagreement is centered around the question on how strong is the influence of the slow nuclear motion on the dynamics of electronic density. Extensive *ab initio* calculations for several molecules [11,12] demonstrated that the nuclear dynamics leads to the decoherence of the electronic wave packet on the timescale of a few femtoseconds, which can make experimental observations

of the electronic motion impossible. At the same time, long-lasting electronic coherences were reported for the ionized propiolic acid [13] and iodoacetylene [14], suggesting that the influence of nuclear motion on the electronic dynamics is very case specific and requires careful investigation.

Understanding the interplay between the nuclear rearrangement and ultrafast electronic motion requires a concerted description of the electron-nuclear dynamics. Being one of the most powerful approaches for this purpose, the multiconfigurational time-dependent Hartree (MCTDH) method [15–17] was recently applied for describing electronic coherence [11,13]. Although this rigorous technique takes into account all quantum effects, such as tunneling and nonadiabatic transitions, it suffers from exponential scaling and also requires constructing global potential energy surfaces (PESs).

An alternative strategy for simulating coupled electron-nuclear dynamics employs a trajectory-guided Gaussian basis to represent the evolving wave packet and an "on-the-fly" evaluation of the electronic structure. These "direct dynamics" approaches calculate the PESs along trajectories only, thus avoiding the precomputation of globally fitted surfaces, and sample only the relevant regions of the configuration space. Among these methods, the closest in spirit to MCTDH are the variational multi-configurational Gaussians (VMCG) [18–22], but many others exist, ranging from *ab initio* multiple spawning [23] and other Gaussian basis methods [24,25] to more approximate mixed quantum-classical [26,27] and semi-classical [28–30] approaches.

Treating electronic coherence with trajectory-based techniques was pioneered by Bearpark, Robb, and co-workers [31–34] who propagated multiple trajectories representing an initially delocalized wave packet using Ehrenfest approximation. Although this technique captures decoherence due to a superposition of coherent oscillations with different frequencies appearing at the respective nuclear geometries, it completely ignores the decoherence due to the quantum motion of the wave packet resulting in the accumulation of phase along the propagated trajectory. The latter mechanism is referred to as the phase jitter [35] in general literature on quantum decoherence or, more specifically, as dephasing in the case of electron-nuclear processes. Allowing the wave packet to evolve quantum mechanically, dephasing mechanism was taken into account and the electronic coherence upon ionization of a system was simulated in several molecules using the direct dynamics version of VMCG scheme [12] and its Ehrenfest-based variant [36].

Here, we use the thawed Gaussian approximation (TGA) [37–39], one of the simplest semiclassical approaches for molecular dynamics, to evaluate the influence of nuclear motion on the ultrafast electronic dynamics and to find a simple, yet detailed mechanism of decoherence, which is not available in basis set methods such as MCTDH or VMCG. Within the TGA, the nuclear wave function is described by a single Gaussian wave packet whose center follows Hamilton's equations of motion and whose time-dependent width and phase are propagated using the local harmonic approximation of the PES.

We simulate coupled electron-nuclear dynamics taking place after outervalence ionization of two polyatomic molecules: propiolic acid (HC_2COOH) and its amide derivative propiolamide (HC_2CONH_2). Propiolic acid provides us a perfect system for validating the semiclassical TGA because the electronic coherences in this molecule were recently calculated using a full quantum MCTDH approach [13]. The propiolamide molecule, in turn, is studied here for the first time.

The starting point of our investigations is a neutral molecule in its ground electronic and vibrational states. The ionization of the system performed by the ultrashort laser pulse can bring the molecule to a nonstationary superposition of ionic states, thus launching a coupled dynamics of electronic and nuclear wave packets. A coherent superposition of multiple electronic states triggers oscillations of the charge along a molecular chain. This purely electronic mechanism was termed "charge migration" [40–43] to distinguish it from a more common charge transfer driven by nuclei [44]. Although the charge migration is governed by the electronic motion, it is strongly coupled with the nuclear dynamics and therefore can crucially affect the behavior of the whole molecule.

Previous calculations of the ionization spectrum of propiolic acid showed [13,45] that, due to the electron correlation, the ground and the second excited ionic states

of the molecule are a strong mixture of two one-hole configurations: an electron missing in the highest occupied molecular orbital (HOMO) and an electron missing in the HOMO-2. Therefore, a sudden removal of an electron either from HOMO or from HOMO-2 will create an electronic wave packet, which will initiate charge migration oscillations between the carbon triple bond and the carbonyl oxygen with a period of about 6.2 fs, determined by the energy gap between the first and the third cationic states [45]. Due to the planar geometry of the propiolic acid and a large energy gap between remaining ionic states, the indicated superposition can be obtained in an experiment by an appropriate orientation of the molecule with respect to the laser polarization.

To describe the ionization process, we used the non-Dyson algebraic diagrammatic construction (ADC) scheme [46] to represent the one-particle Green's function. We chose a rather computationally expensive ADC method because it allows treating the ionization process explicitly starting from the neutral state of a system. This important advantage over other, more conventional electronic structure approaches allows us to estimate populations of the resulting ionic states created after removal of an electron from a molecule. (See Sec. I of the Supplemental Material [47] for details, which includes Refs. [48–51].)

Within the sudden and Franck-Condon approximations, the ionization is modeled by projecting the ground (electronic and nuclear) neutral state of a molecule onto the ionic subspace of the system. After ionization, a single nuclear Gaussian wave packet on each involved ionic surface is propagated independently from the others (nonadiabatic effects are neglected). The center of each Gaussian is guided by a single classical trajectory, while the width and phase are propagated using the single-Hessian [52] variant of the TGA.

Within the Born-Huang representation [53] of the molecular wave function, the expectation value of an electronic operator $\hat{O}(\mathbf{r}, \mathbf{R})$ can be expressed as

$$\langle \hat{O} \rangle(t) = \sum_{i,j} \int \chi_i^*(\mathbf{R}, t) O_{ij}(\mathbf{R}) \chi_j(\mathbf{R}, t) d\mathbf{R}, \quad (1)$$

where $O_{ij}(\mathbf{R}) = \int \Phi_i^*(\mathbf{r}, \mathbf{R}) \hat{O}(\mathbf{r}, \mathbf{R}) \Phi_j(\mathbf{r}, \mathbf{R}) d\mathbf{r}$ denote the $\mathbf{R}$-dependent matrix elements of the electronic operator between electronic states i and j, and the quantities $\chi_i(\mathbf{R}, t)$ are the time-dependent nuclear wave packets propagated on the corresponding PESs.

If both the operator $\hat{O}(\mathbf{r}, \mathbf{R})$ and the electronic states $\{\Phi_i(\mathbf{r}, \mathbf{R})\}$ depend weakly on nuclear coordinates $\mathbf{R}$, Eq. (1) can be further simplified as

$$\langle \hat{O} \rangle(t) \approx \sum_{i,j} O_{ij} \chi_{ij}(t), \quad (2)$$

where the nuclear overlaps $\chi_{ij}(t) = \int \chi_i^*(\mathbf{R}, t) \chi_j(\mathbf{R}, t) d\mathbf{R}$ represent the populations of electronic states when $i = j$
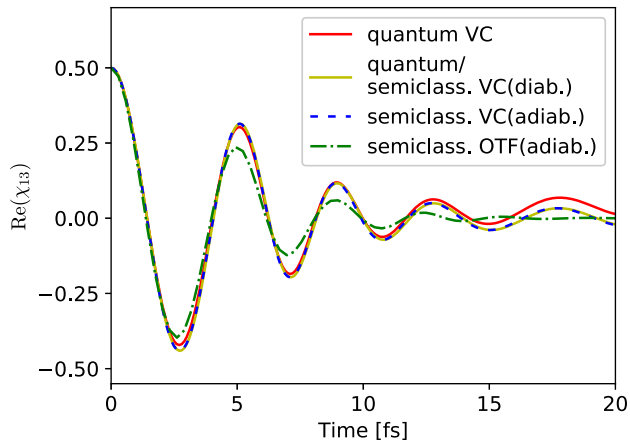
FIG. 1. Electronic coherence measured by the time-dependent overlap $\chi_{13}(t)$ of the nuclear wave packets propagated on the first and third cationic states of propiolic acid after removal of a HOMO electron. Dynamics was performed with the full quantum MCTDH method ("quantum") or with the semiclassical vertical-Hessian thawed Gaussian approximation ("semiclass."), and either with the vibronic coupling ("VC") or on-the-fly ("OTF") Hamiltonian, both obtained at the *ab initio* many-body Green's function ADC(3) level of theory. All simulations except the "quantum VC" calculation employed the diabatic approximation ("diab."), which neglects nonadiabatic couplings between the diabatic states, or the adiabatic approximation ("adiab."), which neglects nonadiabatic couplings between adiabatic states.

and the electronic coherences [11–13] when $i \neq j$. Equation (2) shows that the factors $\chi_{ij}(t)$ provide the only source of time dependence in the expectation value of the electronic operator and thus can serve as convenient properties to quantify the decoherence time. Electronic coherence evaluated as the nuclear overlap $\chi_{ij}(t)$ is a special case of *fidelity amplitude* (also called a Loschmidt echo), a quantity measuring sensitivity of quantum dynamics to perturbations and defined as the overlap at time t of two wave packets, initially the same but propagated with different Hamiltonians [54–61].

We computed the electronic coherences $\chi_{ij}(t)$ generated after ionizing an electron from the HOMO of the propiolic acid; the initial molecular wave packet was an equally weighted and phase-synchronized superposition of the first and third cationic states. Figure 1 shows the electronic coherence evaluated by five different schemes. We adopted the vibronic-coupling (VC) Hamiltonian from Ref. [13] to perform MCTDH simulations taking into account all nuclear degrees of freedom. The full quantum-mechanical calculations show (red solid line in Fig. 1) that the electronic oscillations are strongly influenced by nuclear motion—the coherences are completely suppressed within first 15 fs [13].

To validate the applicability of the TGA, we performed semiclassical calculations using *adiabatic* version of the VC Hamiltonian, where the PESs were obtained by diagonalizing the four-state VC model used in the MCTDH

calculations. Our simulation shows (blue dashed line in Fig. 1) that on the short timescale the TGA gives results almost identical to the full quantum MCTDH calculations. The small deviations start to appear at longer times due to the nonadiabatic effects, neglected in the TGA. Note that TGA is exact within the VC model when the diabatic PESs are not coupled to each other, and therefore provides results identical to the MCTDH simulations performed on such VC Hamiltonian (yellow solid line in Fig. 1).

We also performed semiclassical calculations with on-the-fly evaluation of the electronic structure at the same *ab initio* level of theory as that used in the construction of the VC Hamiltonian (green dash-dotted line in Fig. 1). In this case, the wave packet can potentially evolve beyond a simple model used for fitting PESs. In particular, a VC Hamiltonian typically uses a rather primitive approximation of PESs for nuclear configurations formed by superposition of normal modes. Allowing the wave packet to evolve according to the exact Hamiltonian computed on the fly makes it possible to visit nuclear regions inaccessible within the VC Hamiltonian and thus to take anharmonicity effects into account (see Sec. II of [47] for details). This is reflected in our on-the-fly calculations, which predict the electronic motion with a similar oscillation period, but a slightly faster decay of the electronic coherence than within the VC model. Remarkably, because the effect of using the on-the-fly potential is much larger than the effect of including the nonadiabatic couplings, the semiclassical on-the-fly result of the TGA is most likely more accurate than the quantum result of the MCTDH calculation with the VC model!

In Sec. III of [47], we derive an analytical expression,

$$\chi_{ij}(t) = e^{-d(t)^2/4\hbar} e^{iS(t)/\hbar}, \quad (3)$$

for the semiclassically evaluated coherence in case the two Gaussians have fixed widths. Here $d(t)$ is phase-space distance (in mass- and frequency-scaled phase-space coordinates $\mathbf{R}$ and $\mathbf{P}$) between the centers of the two Gaussian wave packets at time t,

$$S(t) = S_{\text{red}}(t) - \Delta E t, \quad (4)$$

is the classical action, $\Delta E = V_j(\mathbf{R}_0) - V_i(\mathbf{R}_0)$ is the energy gap at the initial point $\mathbf{R}_0$, and

$$S_{\text{red}}(t) = \oint_{\mathbf{C}} \mathbf{P}^T \cdot d\mathbf{R} \quad (5)$$

is the reduced action equal to the signed area within the closed curve $\mathbf{C}$ shown in Fig. 2 [60].

The analytical expression (3) provides a simple, semiclassical interpretation of the effect of nuclear dynamics on electronic coherence (see Fig. 3): the diverging nuclear trajectories affect not only the absolute value of $\chi_{ij}(t)$—which, as expected, decays as a Gaussian function of the
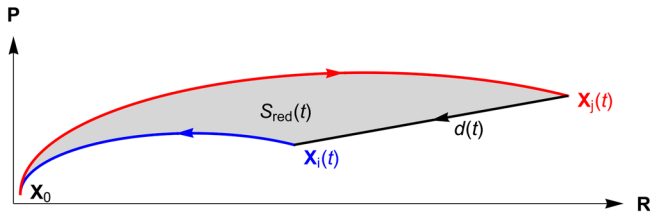
FIG. 2. Geometric interpretation of Eq. (5). The reduced action S_{red} is the gray phase-space area enclosed by the curve **C** consisting of the classical trajectory propagated in state i with potential energy V_i and connecting $\mathbf{X}_i(t)$ with $\mathbf{X}_0$ (blue curve), classical trajectory propagated in state j with potential energy V_j and connecting $\mathbf{X}_0$ with $\mathbf{X}_j(t)$ (red curve), and a straight (black) line connecting $\mathbf{X}_j(t)$ with $\mathbf{X}_i(t)$. The correct sign of S_{red} is obtained by taking the curve integral along **C** in the direction indicated by the arrows. The phase space distance between the final points $\mathbf{X}_j(t)$ and $\mathbf{X}_i(t)$, given by the length d of the black line segment, determines the coherence decay (i.e., the decay of $|\chi_{ij}(t)|$), while the reduced action S_{red}, equal to the gray area, affects the frequency of oscillations of the coherence $\chi_{ij}(t)$.

phase-space distance $d(t)$—but also the frequency of electronic oscillations. In the absence of nuclear motion, the electronic coherence would oscillate with frequency $\Delta E/\hbar$, but now, due to nuclear dynamics, the phase of electronic oscillations at time t is modified by the area $S_{\text{red}}(t)$ divided by $\hbar$ [see Eqs. (3)–(5)]. It is easy to see that if the potential energy surfaces are simply vertically shifted, i.e., if $V_j = V_i + \Delta E$, then $\mathbf{X}_i = \mathbf{X}_j$ and $d = S_{\text{red}} = 0$, implying that the electronic coherence $\chi_{ij}(t)$ is not affected by nuclear dynamics.

Let us turn to the electron-nuclear dynamics driven by the ionization of the propiolamide. Similar to the spectrum

of the propiolic acid [45], in the energy range 10–14 eV only the four states shown in Fig. 2 in Sec. IV of [47] are present. The strong electron correlation between valence orbitals in the neutral propiolamide leads to appearance of the almost equal in weights one-hole configurations in the ionic states. Therefore, an ultrashort (sudden) ionization of the molecule will inevitably create an electronic wave packet and trigger dynamics of the electron density between the carbon triple bond and amide moiety. The molecule is planar and thus belongs to the C_s symmetry group which allows assignment of the ionic states to two irreducible representations: the second and fourth states belong to the A', while the first and third states to A''. As for propiolic acid, orientation of the propiolamide with respect to the polarization of the ionizing laser field can be used to populate only the states of interest.

Figure 4 shows the evolution of the electronic coherence in the propiolamide. Taking advantage of the molecular symmetry, we simulate dynamics occurring after removal of the HOMO (populating the first and third cationic states) and HOMO-1 (populating the second and fourth cationic states) electrons. Starting from the equally weighted and phase-matched superposition of the electronic states, in both cases the nuclear motion perturbs electronic oscillations and leads to decoherence. Coherence times of different molecules can be compared using the purity $\text{Tr}[\rho(t)^2]$ [11], where the electronic density matrix $\rho(t)$ is related to the matrix of nuclear overlaps from Eq. (2) by transposition: $\rho_{ij}(t) = \chi_{ji}(t)$. Due to decoherence, the purity decays from the value $\text{Tr}[\rho(0)^2] = 1$ for the initially
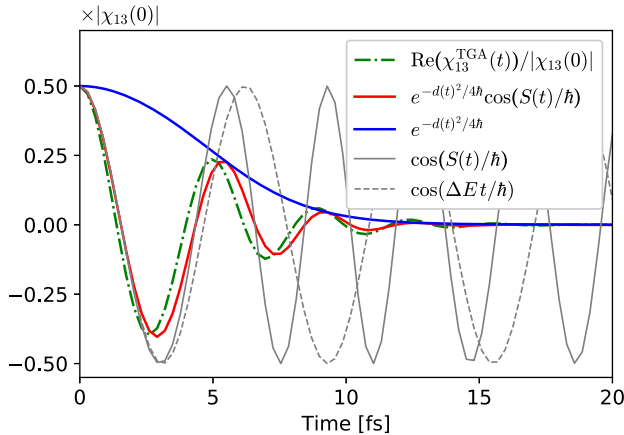

FIG. 3. Semiclassical analysis of the electronic coherence $\chi_{13}(t)$ from Fig. 1. Comparison of the coherence computed with the on-the-fly version of TGA (green dash-dotted line), analytical semiclassical expression (3) (red solid line), factors describing the decay (blue solid line) and oscillations (gray solid line) of coherence in the presence of nuclear motion, and the undamped coherence in the absence of nuclear motion (gray dashed line).
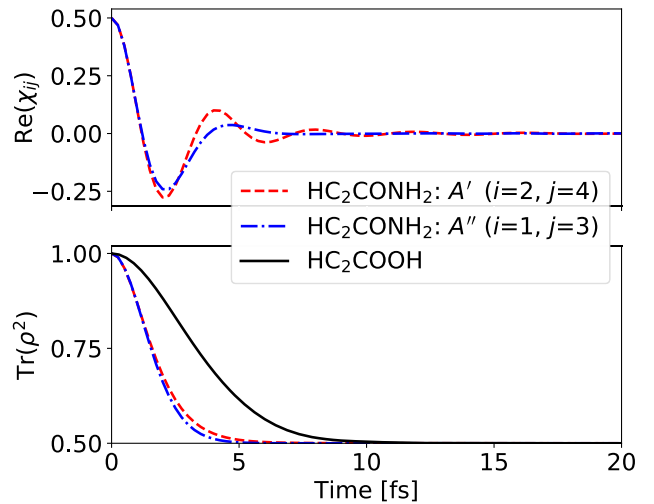

FIG. 4. Top panel: time evolution of the electronic coherences $\chi_{ij}(t)$ created by the equally weighted coherent superposition of the second and fourth cationic states (ionization from the HOMO-1, A' symmetry), and the first and third cationic states (ionization from the HOMO, A'' symmetry). Bottom panel: comparison of the electronic purity function $\text{Tr}(\rho^2)$ for the propiolamide and propiolic acid molecules.

pure state to the value $1/n$ for the equally weighted mixture of n states.

Our simulations demonstrate that, contrary to the propiolic acid molecule, for which long-lasting coherences were observed (see bottom panel of Fig. 4 and also Ref. [13]), the initially pure superpositions in the propiolamide evolve to mixed states in just a few femtoseconds. Importantly, the energy gaps between the involved electronic states of propiolamide are larger than those for the propiolic acid (see Fig. 2 of [47] and Ref. [45]), which leads to faster oscillations of electronic density along the molecular chain. Despite the rather short coherence time, due to the faster charge migration the electronic density in the propiolamide has enough time to perform one clear oscillation (see Fig. 4 above and Fig. 3 of [47]). Moreover, the existence of the strong hole-mixing in both symmetries of the propiolamide can be used to induce oscillations of the charge along different directions in the molecule. Dependence of the charge migration on the molecular orientation provides an important advantage for experimental measurements utilizing the time-resolved high-harmonic generation spectroscopy employed recently by Wörner and coworkers [5]. Alignment of the molecule with respect to the pump pulse should be reflected in the resulting high-harmonic generation spectra and thus can be used as a direct evidence of the ultrafast electron dynamics.

Although trajectory-based direct dynamics methods were previously used to estimate electronic coherences in various polyatomic molecules [12,36], converged results typically required a large number of trajectories. The VMCG used in these studies take into account nonadiabatic transitions and tunneling effects, but require solving rather complicated equations of motion and make interpreting obtained results less intuitive than the simple picture provided here in Eq. (3) and Figs. 2 and 3. Our approach based on the TGA can be viewed as a very special case of far more general VMCG—namely, it can be classified as a single-Gaussian, nonvariational, multiset, nonfrozen, adiabatic, single-Hessian version of VMCG. In contrast to the application of VMCG in Refs. [12,36], our implementation of the TGA uses a multiset approach, where a *single* Gaussian function with *relaxed* parameters is used for every involved electronic state (see also Ref. [62] where accuracy of VMCG with and without relaxation of Gaussian widths is compared). By approximately taking into account quantum properties of the wave packet, such as its width and phase, the TGA captures the dephasing mechanism while maintaining sufficient accuracy, especially at short time scales. A detailed comparison of the TGA and VMCG (calculations are performed using the QUANTICS package [63,64]) is provided in Sec. V of [47]—remarkably, the TGA, which uses only a single classical trajectory per electronic state, yields in the propiolic acid better results than the single-set version of VMCG with 31 variational trajectories (see Fig. 4 in [47]). While the

multiset version of VMCG gives similar results to TGA also with one Gaussian, no improvement is seen by using eight Gaussians (Fig. 4 of [47]). In the TGA, using only two classical trajectories was not only sufficient but also crucial for revealing the simple physical mechanism of decoherence.

The semiclassical vertical-Hessians TGA used in this Letter can be further improved by calculating Hessians along the propagated trajectory and thus taking into account more complicated situations, e.g., dissociation of a molecule. Extensions of the TGA, such as the extended thawed Gaussian approximation [65,66] or Hagedorn wave packets [39,67], which propagate a Gaussian multiplied by a linear or general polynomial, can make on-the-fly semiclassical simulations even more accurate.

In conclusion, we implemented a simple and efficient on-the-fly semiclassical approach to understand the effects of nuclear motion on electronic coherence in molecules. Although the propiolic acid and propiolamide have very similar ionization spectra, our calculations predict that their electronic coherence times differ substantially. The simple method was validated by comparison with the full-dimensional quantum calculations performed using the MCTDH and VMCG methods. As suggested by Fig. 1, neglecting the nonadiabatic couplings by the TGA may not be a severe approximation because, even in systems with strong couplings, the nonadiabatic effects typically start playing a significant role only at times longer than the ultrashort decoherence timescale. If one suspects an exceptional importance of nonadiabatic effects even at times before the electronic coherence has decayed to zero, it is possible to validate the applicability of the TGA without performing expensive quantum simulations by verifying adiabaticity with on-the-fly semiclassical calculations based, e.g., on surface hopping [26] or multiple-surface dephasing representation [68–71].

Despite its limitations, the presented technique for evaluating coherence can help breaking the "curse of dimensionality" appearing in the quantum treatment of large molecules, which can be crucial for full-dimensional simulations of ultrafast electronic processes in biologically relevant systems [72]. Being able to treat molecules with a few hundred atoms, this technique can help shed light on the continuing debates on the role of quantum coherence in biology [73], quickly preselect molecules suitable for further experimental investigations, and support theoretically recent experimental observations of attosecond electron dynamics in realistic molecular systems.

*nik.v.golubev@gmail.com
†jiri.vanicek@epfl.ch

[1] F. Krausz and M. Ivanov, Rev. Mod. Phys. **81**, 163 (2009).
[2] L. Young *et al.*, J. Phys. B **51**, 032003 (2018).
[3] J. Mauritsson, G. Vampa, and C. Vozzi, J. Opt. **20**, 110201 (2018).
[4] F. Krausz, Phys. Scr. **91**, 063011 (2016).
[5] P. M. Kraus, B. Mignolet, D. Baykusheva, A. Rupenyan, L. Horny, E. F. Penka, G. Grassi, O. I. Tolstikhin, J. Schneider, F. Jensen, L. B. Madsen, A. D. Bandrauk, F. Remacle, and H. J. Wörner, Science **350**, 790 (2015).
[6] E. Goulielmakis, Z.-H. Loh, A. Wirth, R. Santra, N. Rohringer, V. S. Yakovlev, S. Zherebtsov, T. Pfeifer, A. M. Azzeer, M. F. Kling, S. R. Leone, and F. Krausz, Nature (London) **466**, 739 (2010).
[7] X. Xie, S. Roither, D. Kartashov, E. Persson, D. G. Arbó, L. Zhang, S. Gräfe, M. S. Schöffler, J. Burgdörfer, A. Baltuška, and M. Kitzler, Phys. Rev. Lett. **108**, 193004 (2012).
[8] F. Lépine, M. Y. Ivanov, and M. J. J. Vrakking, Nat. Photonics **8**, 195 (2014).
[9] F. Calegari, D. Ayuso, A. Trabattoni, L. Belshaw, S. De Camillis, S. Anumula, F. Frassetto, L. Poletto, A. Palacios, P. Decleva, J. B. Greenwood, F. Martin, and M. Nisoli, Science **346**, 336 (2014).
[10] M. Lara-Astiaso, M. Galli, A. Trabattoni, A. Palacios, D. Ayuso, F. Frassetto, L. Poletto, S. De Camillis, J. Greenwood, P. Decleva, I. Tavernelli, F. Calegari, M. Nisoli, and F. Martín, J. Phys. Chem. Lett. **9**, 4570 (2018).
[11] C. Arnold, O. Vendrell, and R. Santra, Phys. Rev. A **95**, 033425 (2017).
[12] M. Vacher, M. J. Bearpark, M. A. Robb, and J. P. Malhado, Phys. Rev. Lett. **118**, 083001 (2017).
[13] V. Despré, N. V. Golubev, and A. I. Kuleff, Phys. Rev. Lett. **121**, 203002 (2018).
[14] D. Jia, J. Manz, and Y. Yang, J. Phys. Chem. Lett. **10**, 4273 (2019).
[15] H.-D. Meyer, U. Manthe, and L. S. Cederbaum, Chem. Phys. Lett. **165**, 73 (1990).
[16] A. Raab, G. A. Worth, H.-D. Meyer, and L. S. Cederbaum, J. Chem. Phys. **110**, 936 (1999).
[17] M. Beck, A. Jäckle, G. Worth, and H.-D. Meyer, Phys. Rep. **324**, 1 (2000).
[18] I. Burghardt, H.-D. Meyer, and L. S. Cederbaum, J. Chem. Phys. **111**, 2927 (1999).
[19] G. A. Worth and I. Burghardt, Chem. Phys. Lett. **368**, 502 (2003).
[20] G. Worth, M. Robb, and B. Lasorne, Mol. Phys. **106**, 2077 (2008).
[21] M. Šulc, H. Hernández, T. J. Martínez, and J. Vaníček, J. Chem. Phys. **139**, 034112 (2013).
[22] G. Richings, I. Polyak, K. Spinlove, G. Worth, I. Burghardt, and B. Lasorne, Int. Rev. Phys. Chem. **34**, 269 (2015).
[23] B. F. E. Curchod and T. J. Martínez, Chem. Rev. **118**, 3305 (2018).
[24] D. V. Shalashilin and M. S. Child, J. Chem. Phys. **121**, 3563 (2004).
[25] K. Saita and D. V. Shalashilin, J. Chem. Phys. **137**, 22A506 (2012).
[26] J. C. Tully, J. Chem. Phys. **93**, 1061 (1990).
[27] X. Li, J. C. Tully, H. B. Schlegel, and M. J. Frisch, J. Chem. Phys. **123**, 084106 (2005).
[28] M. F. Herman and E. Kluk, Chem. Phys. **91**, 27 (1984).
[29] J. Tatchen and E. Pollak, J. Chem. Phys. **130**, 041103 (2009).
[30] M. Ceotto, S. Atahan, G. F. Tantardini, and A. Aspuru-Guzik, J. Chem. Phys. **130**, 234113 (2009).
[31] M. Vacher, D. Mendive-Tapia, M. J. Bearpark, and M. A. Robb, J. Chem. Phys. **142**, 094105 (2015).
[32] M. Vacher, L. Steinberg, A. J. Jenkins, M. J. Bearpark, and M. A. Robb, Phys. Rev. A **92**, 040502(R) (2015).
[33] A. J. Jenkins, M. Vacher, M. J. Bearpark, and M. A. Robb, J. Chem. Phys. **144**, 104110 (2016).
[34] A. J. Jenkins, M. Vacher, R. M. Twidale, M. J. Bearpark, and M. A. Robb, J. Chem. Phys. **145**, 164103 (2016).
[35] G. A. Fiete and E. J. Heller, Phys. Rev. A **68**, 022112 (2003).
[36] A. J. Jenkins, K. E. Spinlove, M. Vacher, G. A. Worth, and M. A. Robb, J. Chem. Phys. **149**, 094108 (2018).
[37] E. J. Heller, J. Chem. Phys. **62**, 1544 (1975).
[38] T. Begušić, J. Roulet, and J. Vaníček, J. Chem. Phys. **149**, 244115 (2018).
[39] C. Lasser and C. Lubich, arXiv:2002.00624.
[40] L. Cederbaum and J. Zobeley, Chem. Phys. Lett. **307**, 205 (1999).
[41] A. I. Kuleff and L. S. Cederbaum, J. Phys. B **47**, 124002 (2014).
[42] J. Breidbach and L. S. Cederbaum, J. Chem. Phys. **118**, 3983 (2003).
[43] A. I. Kuleff, J. Breidbach, and L. S. Cederbaum, J. Chem. Phys. **123**, 044111 (2005).
[44] S. Sun, B. Mignolet, L. Fan, W. Li, R. D. Levine, and F. Remacle, J. Phys. Chem. A **121**, 1442 (2017).
[45] N. V. Golubev, V. Despré, and A. I. Kuleff, J. Mod. Opt. **64**, 1031 (2017).
[46] J. Schirmer, A. B. Trofimov, and G. Stelter, J. Chem. Phys. **109**, 4734 (1998).
[47] See the Supplemental Material at http://link.aps.org/supplemental/10.1103/PhysRevLett.125.083001 for more details.
[48] A. Canal Neto, E. Muniz, R. Centoducatte, and F. Jorge, J. Mol. Struct. THEOCHEM **718**, 219 (2005).
[49] P. Hohenberg and W. Kohn, Phys. Rev. **136**, B864 (1964).
[50] P. J. Stephens, F. J. Devlin, C. F. Chabalowski, and M. J. Frisch, J. Phys. Chem. **98**, 11623 (1994).
[51] M. J. Frisch *et al.*, *Gaussian 16 Revision C.01* (Gaussian Inc., Wallingford, CT, 2016).
[52] T. Begušić, M. Cordova, and J. Vaníček, J. Chem. Phys. **150**, 154117 (2019).
[53] M. Born and K. Huang, *Dynamical Theory of Crystal Lattices*, Oxford Classic Texts in the Physical Sciences (Oxford University Press, Oxford, 1954).
[54] A. Peres, Phys. Rev. A **30**, 1610 (1984).
[55] R. A. Jalabert and H. M. Pastawski, Phys. Rev. Lett. **86**, 2490 (2001).
[56] J. Vaníček, Phys. Rev. E **73**, 046204 (2006).
[57] T. Gorin, T. Prosen, T. H. Seligman, and M. Žnidarič, Phys. Rep. **435**, 33 (2006).
[58] P. Jacquod and C. Petitjean, Adv. Phys. **58**, 67 (2009).

[59] C. Mollica and J. Vaníček, Phys. Rev. Lett. **107,** 214101 (2011).

[60] E. Zambrano and A. M. Ozorio de Almeida, Phys. Rev. E **84,** 045201(R) (2011).

[61] A. Goussev, R. A. Jalabert, H. M. Pastawski, and D. Wisniacki, Scholarpedia **7,** 11687 (2012).

[62] S. Han, D. Xie, and H. Guo, J. Chem. Theory Comput. **14,** 5527 (2018).

[63] G. A. Worth, K. Giri, G. W. Richings, I. Burghardt, M. H. Beck, A. Jäckle, and H.-D. Meyer, The QUANTICS Package, Version 1.1, (University of Birmingham, Birmingham, 2015).

[64] G. Worth, Comput. Phys. Commun. **248,** 107040 (2020).

[65] S.-Y. Lee and E. J. Heller, J. Chem. Phys. **76,** 3035 (1982).

[66] A. Patoz, T. Begušić, and J. Vaníček, J. Phys. Chem. Lett. **9,** 2367 (2018).

[67] G. A. Hagedorn, Ann. Phys. (N.Y.) **269,** 77 (1998).

[68] T. Zimmermann and J. Vaníček, J. Chem. Phys. **132,** 241101 (2010).

[69] T. Zimmermann and J. Vaníček, J. Chem. Phys. **136,** 094106 (2012).

[70] T. Zimmermann and J. Vaníček, J. Chem. Phys. **137,** 22A516 (2012).

[71] A. Prlj, T. Begušić, Z. T. Zhang, G. C. Fish, M. Wehrle, T. Zimmermann, S. Choi, J. Roulet, J.-E. Moser, and J. Vaníček, J. Chem. Theory Comput. **16,** 2617 (2020).

[72] F. Calegari, A. Trabattoni, A. Palacios, D. Ayuso, M. C. Castrovilli, J. B. Greenwood, P. Decleva, F. Martín, and M. Nisoli, J. Phys. B **49,** 142001 (2016).

[73] N. Lambert, Y.-N. Chen, Y.-C. Cheng, C.-M. Li, G.-Y. Chen, and F. Nori, Nat. Phys. **9,** 10 (2013).